High Power Density Adjustable Speed Drive Topology with Medium Frequency Transformer Isolation

José Juan Sandoval* *Student Member, IEEE*
Harish Krishnamoorthy* *Member, IEEE*
Prasad Enjeti* *Fellow, IEEE*
Sewan Choi** *Senior Member, IEEE*

*Department of Electrical & Computer Engineering, Texas A&M University, College Station, USA
**Department of Electrical and Information Engineering, Seoul National University of Science and Technology

***Abstract*— This paper presents a new adjustable speed drive (ASD) topology that employs medium frequency (MF) transformer isolation. The proposed system consists of a new 3-phase push-pull based AC to DC rectifier with a MF AC link employing only two active switches. A single 5-limb multi-winding MF transformer is employed for isolation. The secondary side of the transformer is connected in a zig-zag configuration and is fed to 3-phase diode rectifiers, realizing 12-pulse rectifier operation. The advantages of the proposed system include high power density due to MF transformer isolation, low active switch count, and a simple modulation scheme. Furthermore, zig-zag transformer connection helps to balance leakage inductance on the secondary side. A 690 V_{LL}, 100 HP design example, detailed analysis and extended simulation results are presented to validate the performance of the proposed approach.**

Keywords—adjustable speed drive, multi-winding medium frequency transformer, power density;

I. INTRODUCTION

Electric motors are widely used in industrial, commercial, and residential applications. In fact, it is estimated that electric motors consume 50% to 66% of all electricity generated in the United States [1]. Such motors are usually controlled by adjustable speed drive (ASD) systems in an effort to reduce energy consumption and to process the energy more efficiently. ASD systems are used to reduce energy losses in rotating equipment such as pumps, fans, and compressors [2]. In particular, medium voltage adjustable speed drive (MV-ASD) systems have found extensive application in the petrochemical, cement, and manufacturing industries [3].

The architecture of conventional and commercially available MV-ASD systems (see Fig.1) consists of the following components: line-frequency multi-winding transformer for isolation, 12-pulse or 18-pulse diode bridge rectification, and a simple or neutral point clamped (NPC) inverter [4, 5]. These systems are usually large in size and weight with the magnetics of line-frequency transformers being the major limiting factor. Existing literature has shown that the power density of MV-ASD systems can be improved by employing medium frequency (MF) transformer isolation, effectively decreasing size/weight.

Various MV-ASD systems which employ medium/high frequency isolation and have improved power density are introduced in [6-7]. These systems use medium voltage multi-level converters for AC-DC conversion. Nevertheless, they employ a high number of active switches and have complicated modulation/control schemes. Matrix converter based MV systems are presented in [8-9]. Despite the improvement in input current quality, matrix converter systems still have the issue of using a high number of active switches and employ complicated modulation strategies to avoid current commutation problems. A multi-pulse rectifier approach with star-delta transformer winding was proposed in [10]. The star-delta windings have different turns-ratio causing issues due to unbalanced leakage inductance on the secondary side.

Zig-zag connected medium (alternately, 'high') frequency solid-state transformer (SST) based topology for an 18-pulse rectifier was introduced in [10]. The proposed topology in Fig. 2 seeks to improve over the existing 12-pulse ASD systems through a zig-zag connected MF transformer based push-pull configuration, which has a reduced active switch count and simple modulation strategy. The advantages of the proposed system architecture are the following:

- Only two active switches are employed to perform AC-DC conversion contributing to a low active switch count.
- The use of MF transformer isolation increases power density by reducing the weight/size of the system [10].
- Retrofit replacement of bulky line frequency transformer with MF based transformer front-end is possible with the proposed approach.
- Zig-zag arrangement helps to balance leakage inductance in the transformer secondary windings.
- The control scheme works with simple MF open loop square wave modulation.
- The DC-link voltage can be regulated with duty cycle control. This feature can mitigate nuisance tripping due to voltage swells and capacitor switching transients.

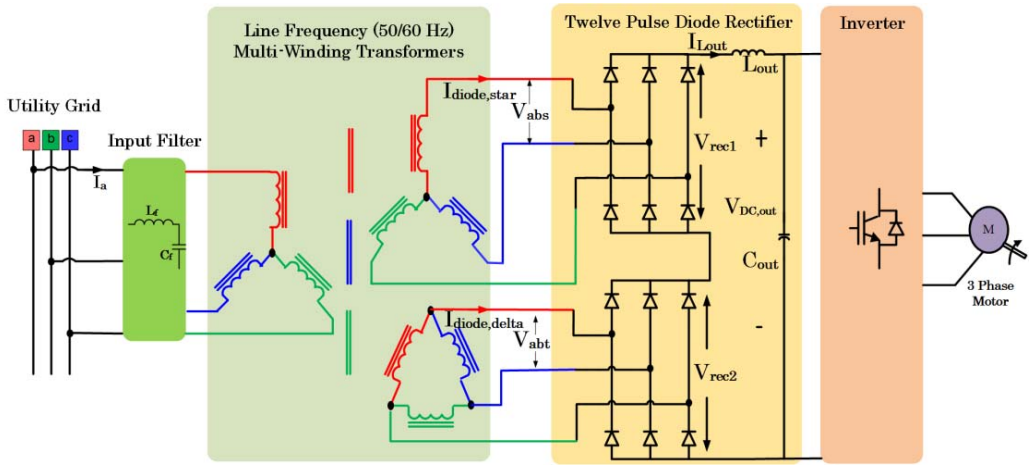

Figure 1: Conventional adjustable speed drive (ASD) system with line frequency isolation transformer and 12-pulse rectifier front-end.

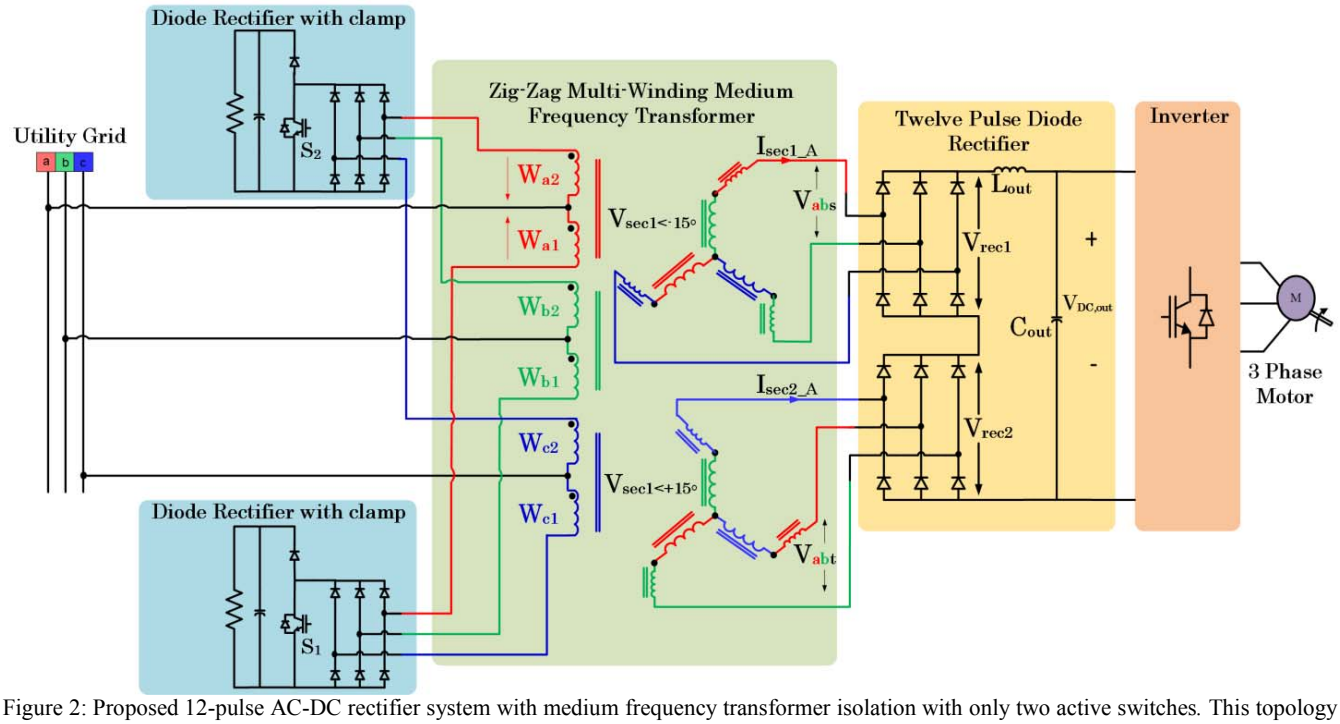

Figure 2: Proposed 12-pulse AC-DC rectifier system with medium frequency transformer isolation with only two active switches. This topology is intended to be a retrofit replacement of typical front-end ASDs. The transformer consists of 5-limbs with three primary windings (with center-tap) and twelve secondary windings.

II. Proposed Medium Frequency Transformer Isolation Based Topology For MV-ASDs

The proposed system employing MF isolation with multi-winding transformers is shown in Fig. 2. Since the focus of this paper is the front-end 12 pulse AC-DC rectifier system, the inverter operation is not explained in much detail. The motor drive inverter can be a simple 3-phase inverter or an NPC inverter. The operation of the proposed topology can be divided in the following stages: (A) diode rectifiers with clamp circuit, (B) MF multi-winding transformer, (C) twelve pulse diode rectifier, and (D) modulation scheme.

A. Diode Rectifiers with Clamp Circuit

This part of the system is composed of two 3-phase diode rectifiers, each connected to a high voltage active switch (S_1/S_2) and a clamp circuit, which consist of a capacitor and a bleeding resistor. The creation of the MF AC link is described in [11]. There are two sets of primary windings (W_{a1}, W_{b1}, W_{c1}) and (W_{a2}, W_{b2}, W_{c2}) which are 180° phase shifted in magnetic coupling. The utility terminals of W_{a1}, W_{b1}, W_{c1} are connected to phase a, b, and c of the utility grid, respectively, while their switching terminals are connected to the diode rectifier with S_1. The utility terminals of windings W_{a2}, W_{b2}, W_{c2} are also connected to the utility grid but their switching

terminals are connected to the diode rectifier with switch S_2. The two switches (S_1, S_2) are complementary and operate at fixed duty cycle. Operation is described for 50% duty cycle.

When S_1 is gated ON and S_2 is gated OFF, the switching terminals of windings (W_{a1}, W_{b1}, W_{c1}) are star connected while the other set of windings (W_{a2}, W_{b2}, W_{c2}) are open. At this moment, since the switching terminals of windings (W_{a1}, W_{b1}, W_{c1}) are star connected, the induced voltages on the secondary side have the same polarity as the utility grid line-to-neutral voltages. Contrastingly, when S_1 is gated OFF and S_2 is gated ON, the switching terminals of windings (W_{a1}, W_{b1}, W_{c1}) are open while the switching terminals of windings (W_{a2}, W_{b2}, W_{c2}) are star connected. At this moment, the induced voltages on the secondary side have opposite polarity compared to the grid line-to-neutral voltages. Since S_1 and S_2 are switched at MF, an AC link is created as shown in Fig. 3. For a switching function given by (1) and a line-to-neutral input voltage as seen by (2), the MF link in V_{Wa1} is given by (3):

$$S_A = \frac{4}{\pi} \sum_{n=1,3,5,\ldots}^{\infty} \frac{1}{n} \sin\left(n\omega_{sqr}t\right) \tag{1}$$

$$V_{an} = \sqrt{\frac{2}{3}} V_{LL} \sin\left(\omega_s t\right) \tag{2}$$

$$V_{Wa1} = \sqrt{\frac{2}{3}} V_{LL} \sum_{n=1,3,5,7,..}^{\infty} \frac{2}{n\pi} \sin(\{n\omega_{sqrt} \pm \omega_s\} \cdot t) \tag{3}$$

The MF link for windings W_{b1} and W_{c1} have the same expression as in (3) but are displaced 120° and 240° respectively.

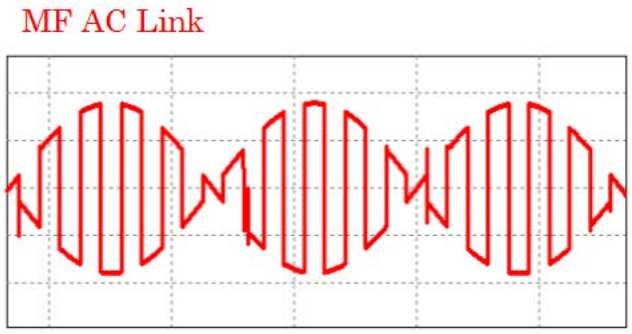

Figure 3: Medium frequency (MF) AC link created by switching S_1 and S_2 complementarily with 50% duty cycle.

When the switching terminals of windings (W_{a1}, W_{b1}, W_{c1}) or (W_{a2}, W_{b2}, W_{c2}) are open, the clamp circuit provides a path for the energy stored in the leakage inductance of the windings. For example, when S_1 is OFF the energy stored in windings (W_{a1}, W_{b1}, W_{c1}) is transferred to the capacitor which clamps to the highest line-to-line voltage. The energy stored in the capacitor can be used to power a switch mode power supply (SMPS). This SMPS can power gate drive circuitry. In this manner, the energy is recovered and not lost in the bleeding resistor.

B. Medium Frequency Multi-Winding Transformer

The switching frequency of S_1 and S_2 determines the operating frequency of the transformer. MF operation enables the transformer to be reduced in size thereby increasing the power density of the system [10]. However, selection of the appropriate magnetic materials is critical to achieve high power density. For high power MF applications, magnetic core materials such as ferrite, amorphous, and silicon steel should be considered [12]. Due to its high saturation flux density and relative low cost [13], a silicon steel core material is selected to build the MF transformers for the scaled down laboratory prototype. Generally, a star-delta winding transformer is used to generate a net 30° phase difference. However, since the turns-ratio is different in star and delta winding configurations leakage inductance balancing issues can occur in the transformer. This problem is mitigated by using zig-zag connection.

The transformer can be three 1-phase multi-winding transformers or it can be a single 3-phase multi-winding transformer. For this system, a single 5-limb transformer is employed for isolation. The primary and secondary windings are wound around the interior 3 limbs of the transformer. The exterior limbs can carry any unbalanced flux in the transformer avoiding core saturation. The 3-phase MF AC links are fed to the primary windings as described in the previous section. The secondary windings are connected in zig-zag arrangement such that two sets of 3-phase voltages result with a phase difference of +15° and -15° with respect to the primary windings (see Fig.4), so that there is a net 30° phase difference between the two sets. To accomplish a net 30° phase difference, the windings turn ratio must be set as given in (4):

$$N_{P1} : N_{P2} : N_{S1} : N_{S2} : N_{S3} : N_{S4} = 1 : 1 : 0.298 : 0.8165 : 0.298 : 0.8165 \tag{4}$$

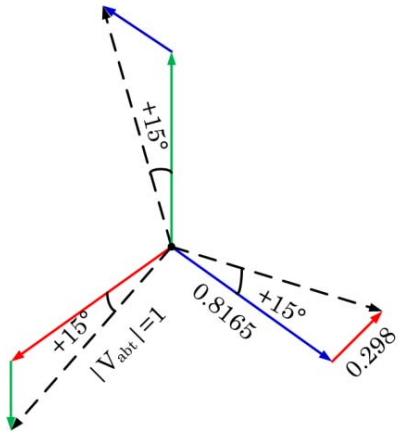

Figure 4: Vector diagram of voltages in zig-zag arrangement. Magnitudes of the vectors can be obtained by phasor operations.

The transformer's turn-ratio can be obtained by performing phasor operations. As shown in Fig. 4, the line-to-line output voltage, V_{abt}, is desired to have a unity magnitude with a phase shift of +15° with respect to the primary line-to-line voltage. Such a vector can be obtained by adding vector V_{an} and the negative of vector V_{bn}. The magnitudes of the vector V_{an} and V_{bn} correspond to the turn ratio of the windings and can be found by solving (5):

$$V_{an}\angle 0° + V_{bn}\angle -120° = 1\angle 15° \quad (5)$$

Breaking (5) into its real and imaginary components yields a system of two equations and two unknowns and therefore the magnitudes of V_{an} and V_{bn} can be obtained. Similar phasor operations can be performed to obtain the magnitudes of the vectors giving a line-to-line output voltage, V_{abs}, with unity magnitude and a phase shift of -15° with respect to the primary line-to-line voltage. The secondary windings of the transformers are connected as shown in Fig. 5. This zig-zag connection yields two set of voltages (V_{abs}, V_{bcs}, V_{cas}) and (V_{abt}, V_{bct}, V_{cat}) which have a 30° phase shift with respect to each other.

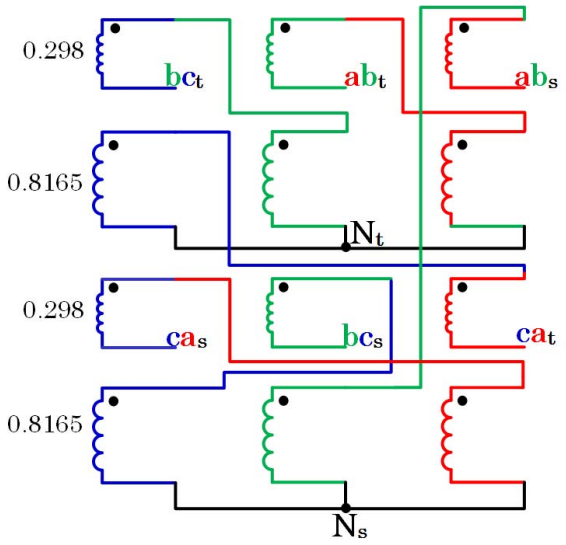

Figure 5: Zig-zag connection of secondary windings. Interior limbs of 3-phase transformer, each limb has four secondary windings.

C. Twelve-Pulse Diode Rectifier

Two sets of 3-phase voltages, with a net 30° phase difference are created with the zig-zag arrangement. Each set is fed to a diode rectifier achieving 12-pulse rectification. The output DC voltage is then interfaced to the inverter. The operation of the bridge rectifiers is similar to the conventional line frequency 12-pulse configuration. The main difference is that fast switching diodes are required for this application. The diodes should be able to switch at the operating frequency. Silicon carbide (SiC) Schottky diodes can be used. These diodes are extremely fast switching and have essentially no reverse recovery current which reduces switching loss [14].

The DC link output voltage, $V_{DC,out}$,of the twelve-pulse diode rectifier is given by (6):

$$V_{DC,out} \approx \frac{6\sqrt{2}}{\pi} V_{abs,rms} \quad (6)$$

The design of the output inductor, L_{out}, and the output capacitor, C_{out}, is similar to the conventional line frequency diode rectifier and depend primarily on the requirements of the motor drive inverter which is not the focus of this paper. The input LC filter is designed similar to the corresponding 12-pulse rectifier's filter since the input currents will have similar harmonic spectrum (*fundamental, 11th, 13th*, etc.)

D. Modulation Scheme

A major advantage of the proposed system is that no closed loop control is required since the topology intends to replicate the performance of a conventional line frequency transformer. The main switches S_1 and S_2 are complementary and operated at fixed 50% duty cycle. Operation at 50% duty cycle provides the maximum MF AC link rms voltage. At duty cycles less than 50%, zero states are introduced to the MF AC link decreasing the overall output DC voltage. If the duty cycle is increased beyond 50%, catastrophic short circuits occur across the transformer windings. Consequently, the modulation becomes simple (open loop fixed duty cycle operation) and robust; in contrast to other systems which employ complicated modulation strategies.

III. Design Example and Simulation Results

A 690 V_{LL}, 100 HP design example is considered to demonstrate the operation of the proposed MV-ASD system in Fig.2. The parameters in Table 1 were used for simulation. Simulations of the proposed topology were performed using PSIM. The simulations were performed without an input LC filter for the sake of clarity. If a filter is desired, it must be designed for a cut-off frequency of 500 Hz (i.e. to eliminate 11th, 13th, and higher harmonics).

As stated in section II, a 3-phase MF AC link is created across the transformer windings by switching S_1 and S_2 complementarily. The 3-phase MF AC link can be observed in Fig. 6(a), it is evident that the voltages across the windings (W_{a1}, W_{b1}, W_{c1}) are displaced by 120° from each other. The voltages across the windings (W_{a2}, W_{b1}, W_{c2}) are also a set of 3-phase voltages with 120° phase shift; however they are opposite in polarity with respect to the voltages across the first set of windings. Fig. 6(b) shows the line-to-line voltages (V_{abs}, V_{abt}) which feed the 12-pulse diode rectifier. The voltages are 30° phase shifted, with respect to each other, as in conventional 12-pulse operation. The input currents to the diode rectifiers, I_{sec1_A} and I_{sec2_A}, in Fig. 6(c) also demonstrate the 30° phase shift. The FFT, Fig. 7, of the voltage across winding W_{a1} confirms MF operation. The fundamental voltage frequency occurs at 400±60 Hz; this enables the use of MF transformers thereby reducing the weight/size of the system [10]. The output DC voltage and the individual rectified

voltages, V_{rec1} and V_{rec2}, are shown in Fig. 8. The 30° phase shift is also noticeable in the individual rectified voltages ensuring 12-pulse operation.

Fig. 9(a) shows the input current for phase a; 12-pulse operation can be observed in the input current. The FFT of the line current is shown in Fig. 9(b); the dominant harmonics are 11^{th}, 13^{th} as in conventional 12-pulse configuration. This shows that the proposed topology can be a retrofit replacement of bulky line frequency transformer based ASD systems.

Table 1: Specification & Operating Conditions used for the system in Fig. 2

Grid voltage (line-to-line rms)	690 V
Rectifier output voltage	1500 V_{dc}
Rated power	100 HP
Square wave switching frequency (f_{sqr})	400 Hz
Output Inductor (L_{out})	2 mH
Output Capacitor (C_{out})	200 µF

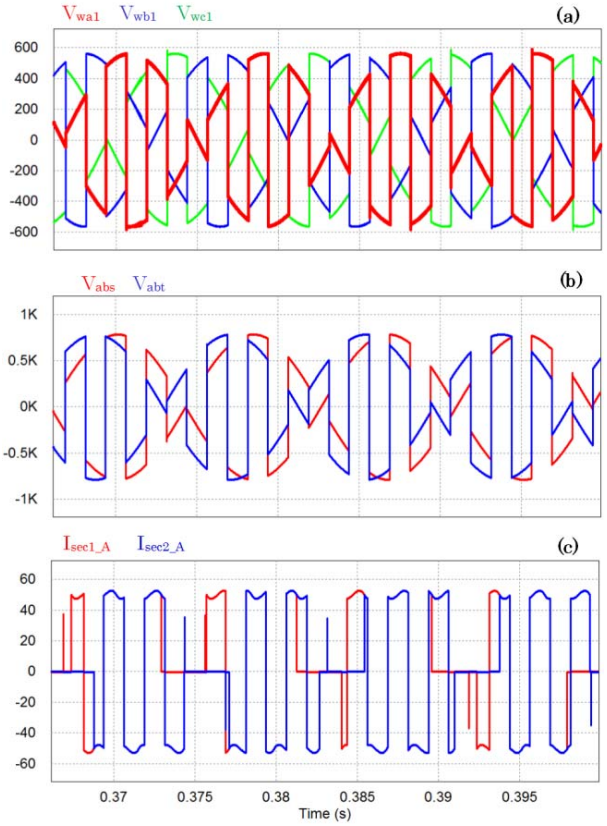

Figure 6: (a) MF 3-phase AC link, the voltages across windings W_{a1}, W_{b1}, W_{c1} are displaced by 120°. (b) Line-to-line voltages V_{abs} and V_{abt}, 30° phase shift between voltages can be observed. (c) Input currents to twelve pulse diode rectifier, 30° phase shift is evident.

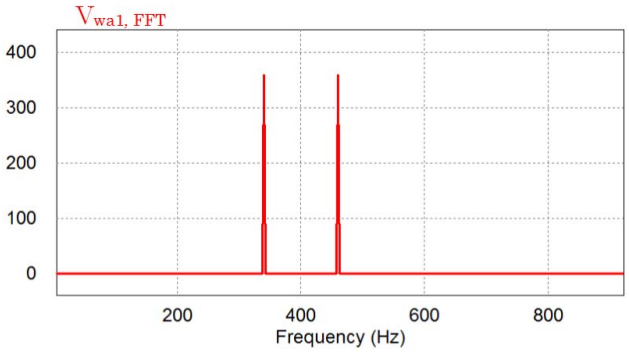

Figure 7: FFT of the voltage across winding W_{a1}. Fundamental frequency of operation is 400±60 Hz enabling the use of MF transformers.

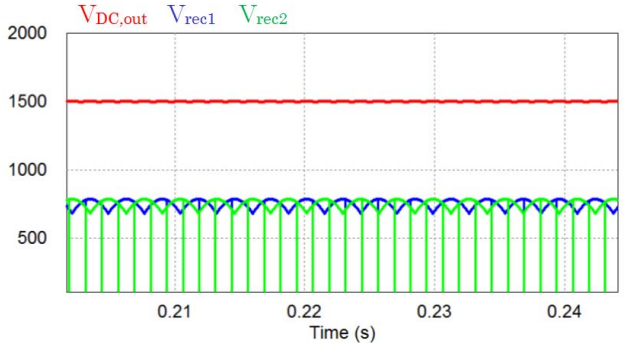

Figure 8: DC output voltage at 1500V. Individual rectified voltages have 30° phase shift as in conventional 12 pulse operation.

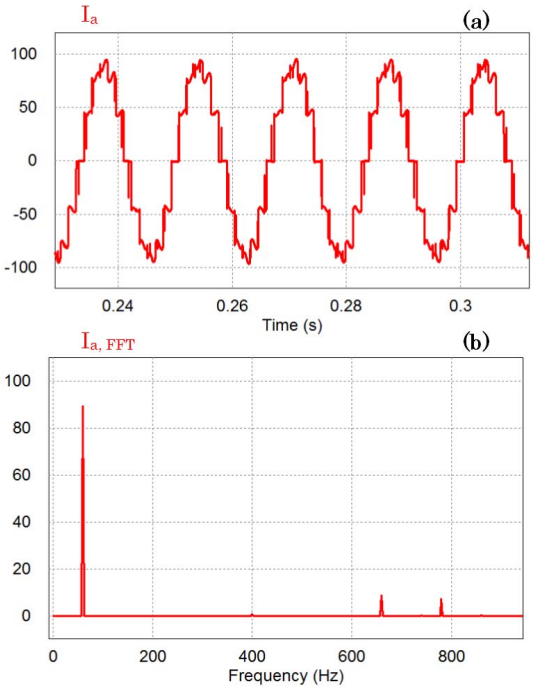

Figure 9: (a) Input line current for phase A; 12-pulse operation can be observed (b) FFT of the input current verifies 12-pulse operation as the dominant harmonics are 11^{th} and 13^{th} (660 Hz and 780 Hz).

IV. Semiconductor Device Count Comparison

A great advantage of the proposed system is that it only employs two high voltage active switches to perform AC-DC conversion. A comparison of the number of semiconductor devices utilized between the system proposed in this paper, the conventional system, and the topologies proposed in existing literature for MV-ASDs is given in Table 2.

Table 2: Comparison of semiconductor devices in MF MV-ASDs' (AC-DC conversion stage)

System Topology	Number of active switches	Number of diodes
Conventional	0	12
[6]	36	0
[10]	12	24
Proposed	2	26

The conventional system uses bulky line frequency transformers and therefore does not utilize active semiconductor devices in the front-end. However, the power density of the system is low. The system in [6] has a higher number of active switches. It is worth noting that this system uses bidirectional multi-level DC-DC converters for 3.3 kV systems using 1.2 kV active switches. The topology in [10] operates at MF, but still has the issue of higher number of active devices. Overall, the proposed topology in this paper has lower number of semiconductor devices used for rectification while achieving high power density. This also results in reduced gate drive circuitry and heat sink utilization. It is worth noting that the two active switches must be rated for twice the line-to-line input voltages. For the ratings in the design example, at least 2 kV active switches must be used.

V. Efficiency Calculation Of AC-DC Conversion Stage

The efficiency of the proposed system can be calculated by analyzing switching and conduction losses, and transformer core and winding losses. Since the focus of this paper is the front-end AC-DC conversion stage of a MV-ASD system, the losses of the motor drive inverter are not included in this analysis. For the proposed design example in section III, the total transformer losses (core and winding losses) are assumed to be approximately 1.5% of the system's power rating. The switching losses and conduction losses of the two high voltage active switches (S_1/S_2) can be approximated by looking at the switching/conducting characteristics of commercially available high voltage IGBTs. The switching loss of the IGBTs and diodes is calculated using the turn-on and turn-off energy pulses of the device as in (7):

$$P_{sw\_loss} = (E_{on} + E_{off}) \cdot f_{sw} \tag{7}$$

The IGBT in [15] is selected for this computation. The conduction losses for this device can be computed by analyzing conduction forward voltage drop and by observing the rms current through the device in simulation. The conduction losses of the two 3-phase diode rectifiers with clamp circuit are calculated using the characteristics of the device in [14] and the average current, obtained from simulation, through the diodes. The switching loss for these diodes is essentially zero as stated in [14]. The losses for the twelve pulse diode rectifiers in the secondary side are obtained in similar manner but using the characteristics of the device in [16]. Table 3 shows the commercial semiconductor devices used for the power loss analysis.

Table 3: Semiconductor devices used for power loss analysis

System Component	Part Number	Manufacturer
S1/S2	IXA40I4000KN	IXYS
3-phase diode clamp circuit	C4D40120D	Cree
Twelve pulse diode rectifier	C3D25170H	Cree

The breakdown of the system losses is shown in Fig. 10. From the analysis it is observed that 41% of the total losses come from the transformer core and winding losses. The assumption of 1.5% transformer loss can be reduced to about 0.5% if more efficient magnetic material like amorphous is used for the transformer design. However, using amorphous material will increase the cost of the transformer. The switching and conduction losses of the active switches in the proposed system account for 16% of the total losses. Since the diodes of the active clamp circuits must also be rated for high voltage, they contribute to 30% of the system losses. Overall, the efficiency of the proposed system is calculated to be 96.4%.

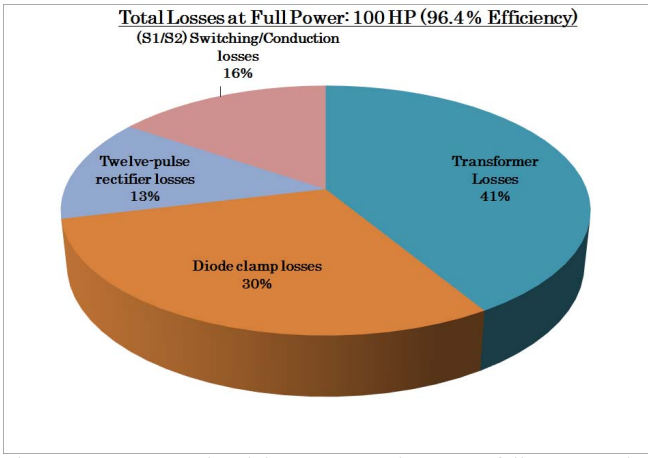

Figure 10: System breakdown power loss. At full power, the efficiency is calculated to be 96.4%.

VI. Conclusion

This paper proposes a MF transformer based push pull topology for ASD systems using only two active semiconductor devices. Using MF transformer isolation increases the power density of the system. Thus, the front-end of this approach can be a retrofit replacement for bulky line frequency transformers in conventional ASDs. The operation of the topology for 12-pulse configuration was described. Zig-

zag arrangement in the secondary side of MF transformer was introduced and derivation of the turns-ratio was shown. Simulation results demonstrate the feasibility of the proposed topology. In addition, power loss analysis of the proposed system yields a 96.4% efficiency at full power using a silicon steel core transformer but this efficiency can be expected to be higher with magnetic core material such as amorphous. Overall, the advantages of the system include high power density, reduced active switch count, and simple open loop control. The zig-zag multi-winding transformer is currently under development.

REFERENCES

[1] Ned Mohan. "Power Electronics and Drives: Enabling Technologies," in *Power Electronics and Drives*, 2003 ed. Minneapolis: MNPERE, 2003, ch.1, sec 1-3-1, pp 1-4.

[2] Hickok, Herbert N., "Adjustable Speed---A Tool for Saving Energy Losses in Pumps, Fans, Blowers, and Compressors," *IEEE Transactions on Industry Applications,* vol.IA-21, no.1, pp.124, 136, Jan. 1985.

[3] Hanna, R.A.; Prabhu, S., "Medium-voltage adjustable-speed drives-users' and manufacturers' experiences," *IEEE Transactions on Industry Applications,* vol.33, no.6, pp.1407, 1415, Nov/Dec 1997.

[4] "Toshiba MV Drives", Available: http://www.toshiba.com/ind/data/tag_files/MTX_NEMA_3R_MV_Brochure_3002.pdf

[5] "TM-GE MV Drives", Available: http://www.wmea.net/Technical%20Papers/GE%20Medium%20Voltage%20Drives.pdf

[6] Inoue, S.; Akagi, H., "A Bidirectional Isolated DC–DC Converter as a Core Circuit of the Next-Generation Medium-Voltage Power Conversion System," *IEEE Transactions on Power Electronics,* , vol.22, no.2, pp.535,542, March 2007.

[7] Heinemann, L., "An actively cooled high power, high frequency transformer with high insulation capability," *Applied Power Electronics Conference and Exposition, 2002. IEEE Seventeenth Annual APEC 2002.*, vol.1, no., pp.352,357 vol.1, 2002.

[8] Jun Kang; Yamamoto, E.; Ikeda, M.; Watanabe, E., "Medium-Voltage Matrix Converter Design Using Cascaded Single-Phase Power Cell Modules," *, IEEE Transactions on Industrial Electronics*, vol.58, no.11, pp.5007,5013, Nov. 2011.

[9] Drabek, P.; Peroutka, Z.; Pittermann, M.; Cédl, M., "New Configuration of Traction Converter With Medium-Frequency Transformer Using Matrix Converters," *IEEE Transactions on Industrial Electronics,* vol.58, no.11, pp.5041,5048, Nov. 2011.

[10] Krishnamoorthy, H.S.; Enjeti, P.N.; Garg, P., "Simplified medium/high frequency transformer isolation approach for multi-pulse diode rectifier front-end adjustable speed drives," *2015 IEEE Applied Power Electronics Conference and Exposition (APEC),* vol., no., pp.527,534, 15-19 March 2015

[11] Gupta, R.K.; Mohapatra, K.K.; Mohan, N., "A novel three-phase switched multi-winding power electronic transformer," *IEEE 2009 Energy Conversion Congress and Exposition, 2009.* vol., no., pp.2696,2703, 20-24 Sept. 2009.

[12] W. M. Colonel and T. Mclyman, *Transformer and Inductor Design Handbook*, 3rd ed. Boca Raton, FL, USA: CRC Press, 2004.

[13] She Xu, A. Q. Huang, and R. Burgos, "Review of Solid-State Transformer Technologies and Their Application in Power Distribution Systems," IEEE Journal of Emerging and Selected Topics in Power Electronics, vol. 1, pp. 186-198, 2013.

[14] Cree Inc, "Silicon Carbide Schottky Diode," C4D40120D datasheet, 2014. Rev. E.

[15] IXYS, "XPT IGBT," IXA40I4000KN datasheet, 2014. Rev.-

[16] Cree Inc, "Silicon Carbide Schottky Diode," C3D25170H datasheet, 2011. Rev.-